

We are IntechOpen, the world's leading publisher of Open Access books Built by scientists, for scientists

6,900

Open access books available

185,000

International authors and editors

200M

Downloads

Our authors are among the

154

Countries delivered to

TOP 1%

most cited scientists

12.2%

Contributors from top 500 universities



WEB OF SCIENCE™

Selection of our books indexed in the Book Citation Index
in Web of Science™ Core Collection (BKCI)

Interested in publishing with us?
Contact book.department@intechopen.com

Numbers displayed above are based on latest data collected.
For more information visit www.intechopen.com



Burst-mode Optical Amplifiers for Passive Optical Networks

Ken-Ichi Suzuki

*NTT Access Service Systems laboratories, NTT Corporation
Japan*

1. Introduction

Passive optical network (PON) systems are being used to create cost-effective optical access network systems (H. Shinohara, 2007) because the central office equipment and the optical transmission fibers can be shared by several customers. To offer PON-based optical access services more economically, the optical line terminal (OLT) installed in the central office must accommodate as many customers as possible and as efficiently as possible. In areas that have relatively lower service demand, it is important to enlarge the transmission distance between the OLT and optical network units (ONUs) in customer premises. In areas that have relatively higher densities, it is important to increase the splitting number of optical splitters. Both actions minimize the need to install additional OLTs in the central office. Enlarging the transmission distance enables remote customers to be serviced while retaining the cost benefits of the PON systems and increasing the splitting ratio enables a system to offer the services to many more urban customers.

To enlarge the transmission distance, we developed a PON repeater or a PON extender box with 3R (reshaping, re-timing, and regenerating) functions (K-I. Suzuki, et al., 2002). However, the 3R functions require a dedicated repeater to be developed for each PON system given that there are various transmission bit-rates and transmission protocols specified in ITU-T Recommendation G.984 series, IEEE 802.3ah, and so on. Therefore, we investigated the use of optical amplifiers as the PON repeaters because these can amplify optical signals regardless of the transmission bit-rate and/or protocol because their amplifications do not require any O/E (optical to electrical) conversion and/or E/O (electrical to optical) conversion. Therefore, we have intensively investigated long-reach PON systems based on optical amplifiers (K-I. Suzuki, et al., R. Davely, et. al., 2009, F. Saliou, et. al., 2009). Moreover, PON-extender boxes were standardized as ITU-T Recommendation G.984.6 to realize long-reach gigabit PON systems.

Figure 1 shows the long-reach PON system with the repeatered system configuration for single fiber WDM (Wavelength Division Multiplexing). In current PON systems, which have been widely installed in the world, upstream and downstream wavelengths lie in the 1.31 μm region and the 1.49 μm region, respectively. Different maximum OLT-ONU distances are specified in different standards but the range is, logically, from 10 to 60 km. Engineering-wise, however, the maximum OLT-ONU transmission distance depends on the splitting loss of the optical splitter and is as short as 7 km with the splitting number of 32 (H. Ueda, et. al., 1999). Moreover, the maximum number of branches continues to increase with

the example being a G-PON with 64 branches (logically up to 128). Basing the PON repeater on optical amplifiers is a promising approach to achieving both longer transmission distances and higher splitting numbers.

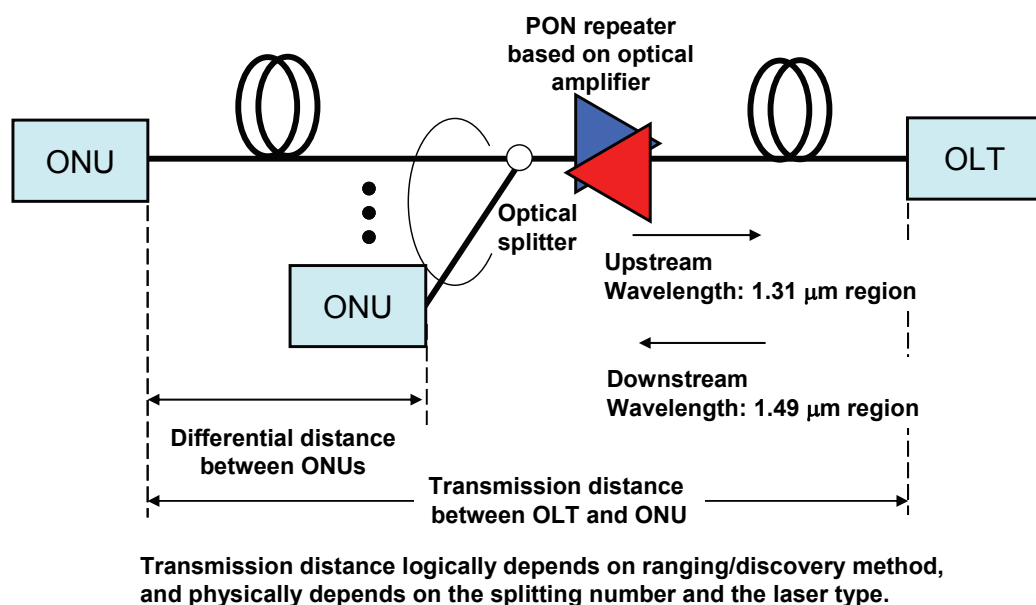


Fig. 1. Long-reach PON system with the repeatered system configuration for single fiber WDM

I next explain the transmission signals in PON systems. As the downstream optical signal is a continuous wave, we can employ an optical amplifier with conventional techniques. In the upstream direction, on the other hand, as the distances between the OLT and each ONU differ, the OLT must be able to receive optical burst signals with different intensities from the ONUs. It is clear that the PON repeater based on optical amplifiers must also be able to amplify these signals without any distortion. However, optical burst signal amplification leads to optical surges as shown in Fig.2, which may well cause failure of the optical receiver as well as interfering with the reception of normal signals at the OLT due to gain dynamics. So we have to use burst-mode optical amplifiers to suppress these optical surges and achieve gain stabilization.

In this chapter, I present burst-mode optical amplifiers for PON systems based on a couple of linear-gain control techniques, gain-clamping (GC) (G. Hoven, 2002, K-I. Suzuki, et. al., 2005), fast automatic gain controlling (fast AGC) (Y. Fukada, et. al., 2008, H. Nagaeda, et. al., 2008), and fast automatic level controlling (fast ALC) (K-I. Suzuki, et. al., 2009) for optical amplifiers. We also discuss the system design based on the signal to noise ratio (SNR) of the long-reach PON systems (K-I. Suzuki, et. al., 2006). On the other hand, 10 Gbit/s class high-speed PON systems have been receiving great attention, which were standardized in IEEE 802.3av and FSAN/ITU-T to cover the future demand, created by the rapid growth of Internet access and IP video delivery services, for high capacity communication. So, I also introduce 10 Gbit/s optical burst signal amplification based on GC optical fiber amplifiers (OFA's) (K-I. Suzuki, et. al., 2008) and optical automatic level control (ALC) techniques applied to fast AGC-OFA's (K-I. Suzuki, et. al., 2009) to ease the requirements of the receiver's dynamic range to confirm their feasibility.

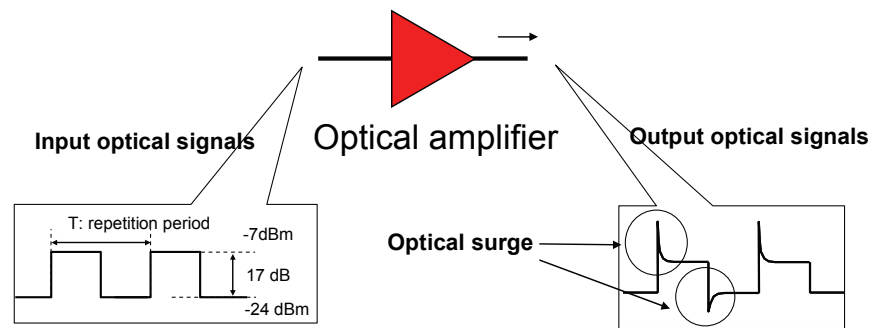


Fig. 2. Optical surge generation

2. Optical surges; Principle of gain-dynamics of optical amplifier

Figures 3 (a)-(b) show optical surges and Fig. 4 shows the numerical and experimental results of normalized optical surge intensity as a function of burst repetition rate ($1/T$) in the case of 1.3 μm fiber optical amplifier using PDFA (Praseodymium-doped fiber amplifier) using the experimental setup shown in Fig. 2. Mark and space levels are set to -7 dBm and -24 dBm, respectively. Gain characteristics are shown as those of PDFA without gain-clamping in Fig. 9 (a). We normalize optical surge intensity using the ratio of optical surge peak level to restored normal signal level in the case of a space to mark level (S-M) transition, see Fig. 3(a). In the case of a mark to space level (M-S) transition, shown in Fig. 3(b), we use the ratio of optical surge bottom level to restored normal signal level. Numerical results were calculated using measured gain relaxation time constants for both transitions. We estimated the gain relaxation time constants as 8.0 μs for S-M transition and 76 μs for M-S transition. Accordingly, we can calculate the gain dynamics $G(t)$ by using the following simple equation.

$$G(t) = G_f + \Delta G \exp(-t / \tau)$$
 (1)

where G_f is the initial gain value at the transition, ΔG is the difference between G_f and the intrinsic gain value for the input signals after the transition, and τ is the gain relaxation time constant. In this case, it takes several hundred micro seconds to restore gain to its normal

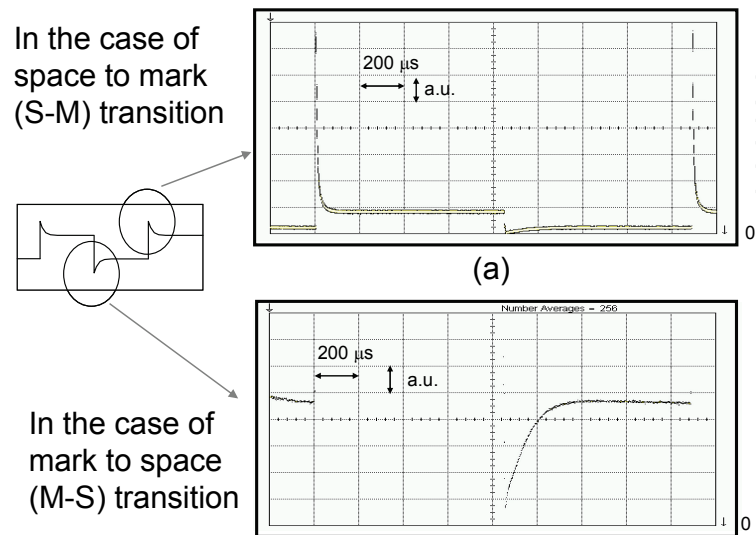


Fig. 3. Optical surges at (a) S-M transition and (b) M-S transition.

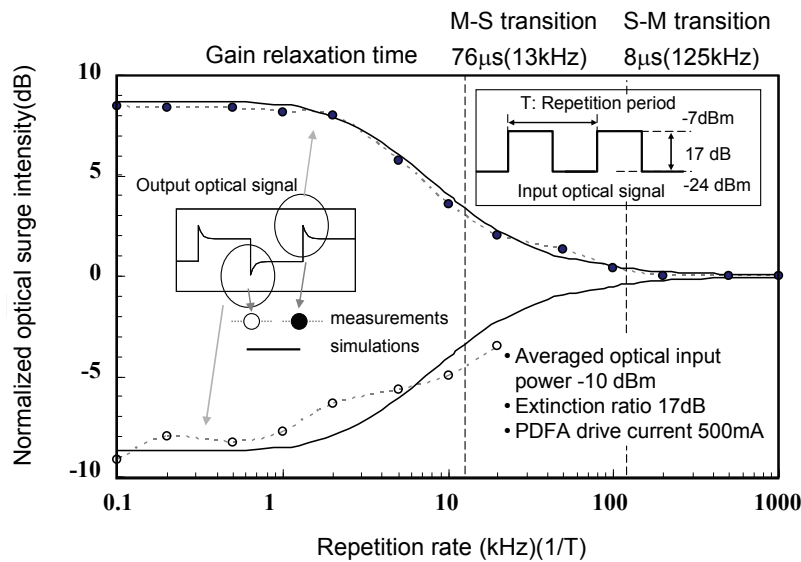


Fig. 4. Numerical and experimental results of normalized optical surge intensity as a function of burst repetition rate.

state because of its large gain relaxation time. Therefore, we adopt numerical values after the calculation becomes a steady state in excess of several hundred micro seconds to well handle repetition periods much smaller than the gain relaxation time.

3. Signal to noise ratio of Long-reach PON system based on optical amplifier

In this section, we confirm the validity of the optical-amplifier for PON systems by estimating the limits placed on the upstream transmission distance (ONU to OLT) in Long-reach PON systems. Figure 5 shows the schematic diagram for the signal to noise ratio (SNR) calculation of a Long-reach PON system consisting of an ONU, an OLT, an optical amplifier with optical splitter and optical fibres. The signal wavelength is 1.31 μm. We assume that the total loss of the 2ⁿ way splitter is 3.5n + 0.5 dB (n is the number of stages in the multistage splitter) because of its 0.5n dB deviation of the splitting ratio (deviation is 0.5 dB/stage) and insertion loss in 0.5 dB in addition to its 2ⁿ way splitting loss of 3.0n dB. For example, the total loss of a 32 way splitter is estimated to be 18 dB.

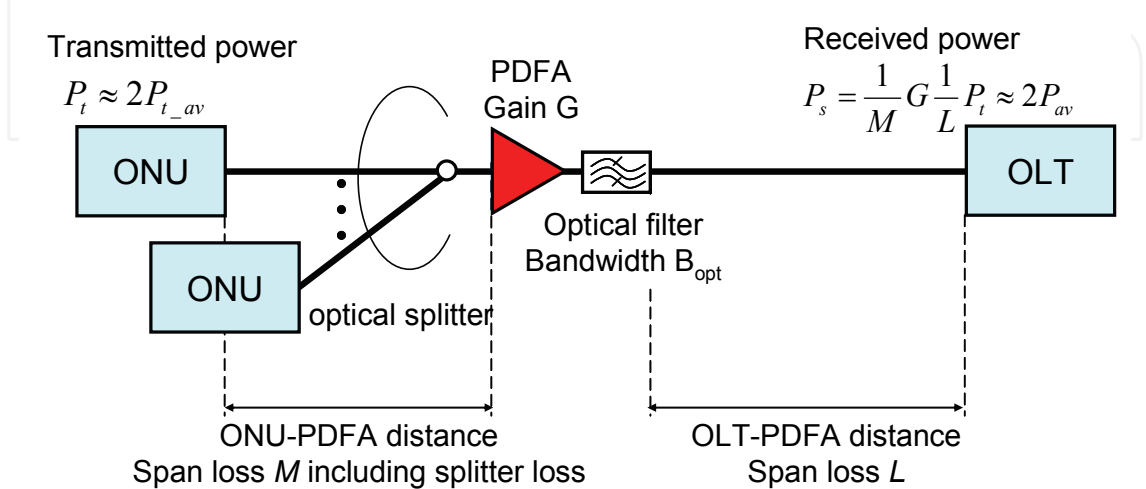


Fig. 5. Schematic diagram for SNR calculation of Long-reach PON system.

No.	Quantity	Symbol	Value	Unit
1	wavelength	λ	1.3	μm
2	Bit rate	B	1.25	Gbit/s
3	quantum efficiency	η	0.8	
4	Equivalent noise current	I_{eq}	5.2	$\text{pA}/\sqrt{\text{Hz}}$
5	inverted population parameter	n_{sp}	2	
6	Gain	G	17	dB
7	Extinction ratio	r	0.1	
8	Fiber loss		0.5	dB/km
9	2^n way optical splitter loss		$3.5n + 0.5$	dB
10	Transmitted power (Averaged transmitted power)	P_t $(P_{t_{av}})$	4 (1)	dBm
11	Filter bandwidth	B_{opt}	3	nm

Table 1. Calculation parameters

Equation (2) was used to calculate SNR of this Long-reach PON system. In a conventional Long-reach PON system based on optical amplifiers, signal-spontaneous beat noise is the dominant problem with regard to receiver sensitivity. However, we also need to consider the circuit noise of the optical receiver because the amplified spontaneous emission (ASE) is reduced due to the fibre loss of the following span in the mid-span repeatered configuration.

$$SNR = \frac{\left(\frac{e\eta}{h\nu}(1-r)P_s\right)^2}{\left(\sqrt{A} + \sqrt{C}\right)^2 \frac{B}{4}}$$

(2)

$$A = e\frac{e\eta}{h\nu}P_s + I_{eq}^2 + \left(\frac{e\eta}{h\nu}\right)^2 2P_s \frac{P_{sp}}{L} + 2\left(\frac{e\eta}{h\nu} \frac{P_{sp}}{L}\right)^2 B_{opt}$$

$$C = e\frac{e\eta}{h\nu}rP_s + I_{eq}^2 + \left(\frac{e\eta}{h\nu}\right)^2 2rP_s \frac{P_{sp}}{L} + 2\left(\frac{e\eta}{h\nu} \frac{P_{sp}}{L}\right)^2 B_{opt}$$

$$P_{sp} = h\nu(G-1)n_{sp}$$

where r is the extinction ratio between mark and space signals, P_s is the optical power of the mark signal (the average power is almost $P_s/2$), B is the bit-rate of the transmission signals, P_{sp} is the frequency density of ASE power of one side of the polarization components, and B_{opt} is the bandwidth of the optical filter used for ASE elimination. G and n_{sp} are the gain and the inverted population parameter of the optical amplifier, respectively. A and C show the noise elements related to the mark and space signals, respectively. The first term of each equation is the shot noise (related to the optical-electrical signal conversion), the second term is the frequency density noise power (related to the equivalent noise current of the receiver front-end circuit), the third term is the signal-spontaneous beat noise, and the forth term is the spontaneous-spontaneous beat noise since we must consider the ASE component

with orthogonal polarization to the optical signals as well as that with the same polarization as the optical signals.

Equation (3) shows the relationship between bit error rate (BER) and Q factor and SNR (N. A. Olsson, 1989, N. S. Bergano, et. al., 1993, T. Takahashi, et. al., 1995).

$$\text{BER} = \frac{1}{\sqrt{\pi}} \frac{\exp\left(-\frac{Q^2}{2}\right)}{Q} \quad (3)$$

where Q is given by:

$$Q = \sqrt{\frac{\text{SNR}}{4}} \quad (4)$$

Therefore, we can obtain the BER using Eqs (2), (3) and (4).

Figures 6(a) and (b) show the SNR values calculated using Eq. (2) as a function of the transmission distance between an OLT and a PDFA with the parameter of ONU-PDFA distance for two filter bandwidths (1 nm and 20 nm). Table 1 shows the calculation parameters. The SNR with 20 nm bandwidth filter is degraded compared as that with the 1 nm filter because of its large spontaneous-spontaneous beat noise. However, we confirmed that over 40 km transmission can be achieved with the relatively wide band-pass filter in 32 way splitting PON systems at the bit-rate of 1.25 Gbit/s.

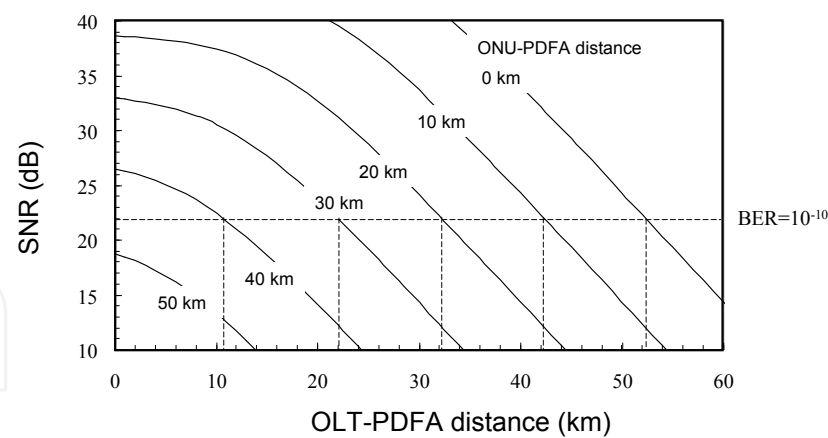
Figure 7 shows SNR as a function of the splitting number; the parameter is the ONU-PDFA distance and the OLT-PDFA distance is fixed at 0 km (i.e., the PDFA is employed as a pre amplifier and the OLT-ONU distance is varied.). As shown in Fig. 7, we find that splitting numbers above 470 are possible at the ONU-PDFA distance of 10 km. Moreover, the splitting number can exceed 630 at the ONU-PDFA distance of 7km.

4. Burst-mode optical amplifier using gain-clamping

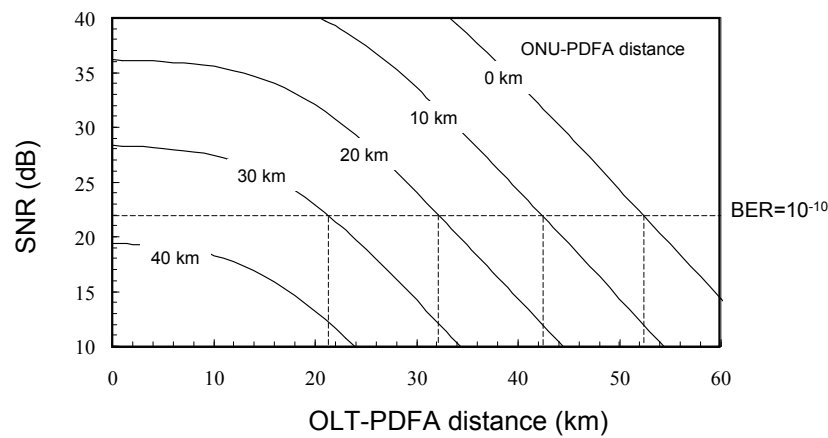
4.1 Gain-clamped Praseodymium-doped fiber amplifier for burst-mode amplification

There are two major gain control methods for optical amplifiers. One is automatic gain control (AGC), which uses feedback/forward gain controls to realize constant gain operation. The other is gain-clamping, which offers constant gain operation using relatively high power control lights compared to optical signals. AGC is being used in the optical repeaters in many long haul transmission systems. However, AGC response time depends on the gain dynamics of the optical amplifiers as well as the speed of the control circuits, so it is impractical to use AGC without any technology progress to handle burst signals. Since gain-clamping is independent of gain dynamics and the control circuit speed (H. Masuda, et. al., 1997; L. L. Yi, et. al., 2003; Yung-Hsin Lu, et. al., 2003; D. A. Francis, et. al., 2001; G. Hoven, 2002), we adopted to realize burst mode amplification in our initial investigation.

In this section, I explain the gain dynamics of PDFAs for designing a burst mode optical amplifier and confirm the gain-clamp effect for burst mode amplification. Figure 8 shows the configuration of a gain-clamped PDFA that supports burst mode amplification. The gain-clamped PDFA consists of two PDFA gain stages pumped by 0.98 μm laser diodes (LD's). The first gain stage uses forward pumping and backward gain-clamping. The second stage uses backward pumping and backward gain-clamping. Forward and backward pumping



(a)



(b)

Fig. 6. SNRs as a function of transmission distance between OLT and PDFA with the parameter of ONU-PDFA distance with parameter of ONU-PDFA distance (a) B_{opt} is 1 nm, (b) B_{opt} is 20 nm.

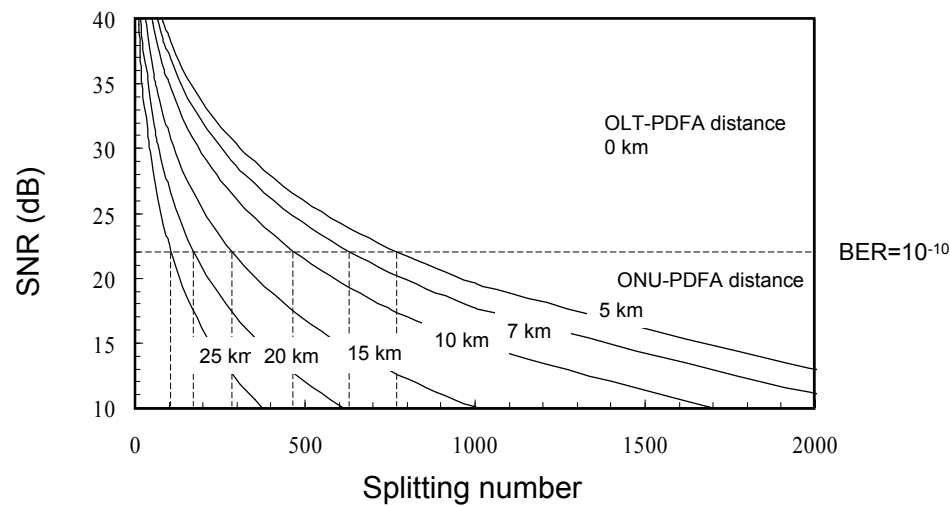


Fig. 7. SNRs as a function of splitting number with the parameter of ONU-PDFA distance and the fixed OLT-PDFA distance of 0 km. and B_{opt} of 20 nm.

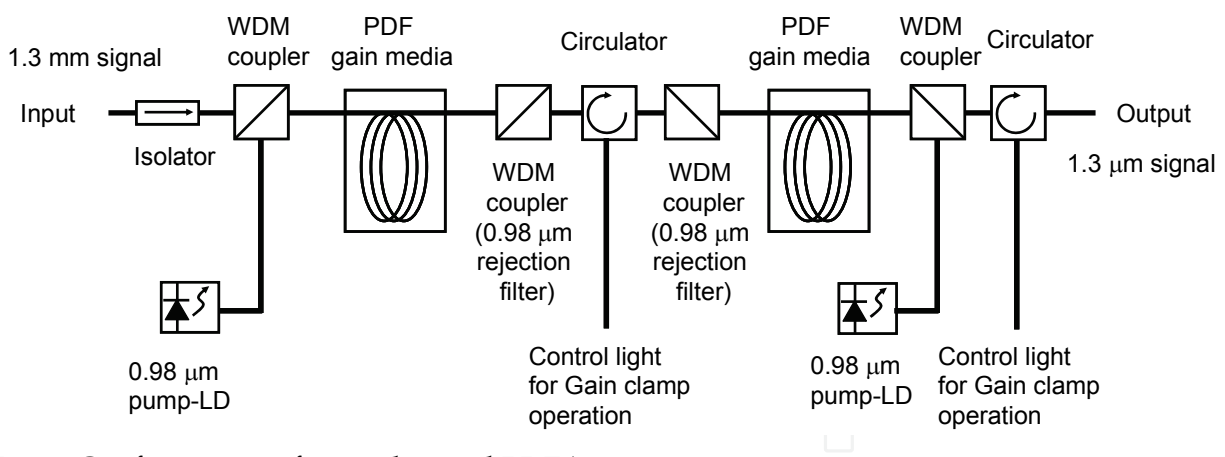


Fig. 8. Configuration of gain-clamped PDFA

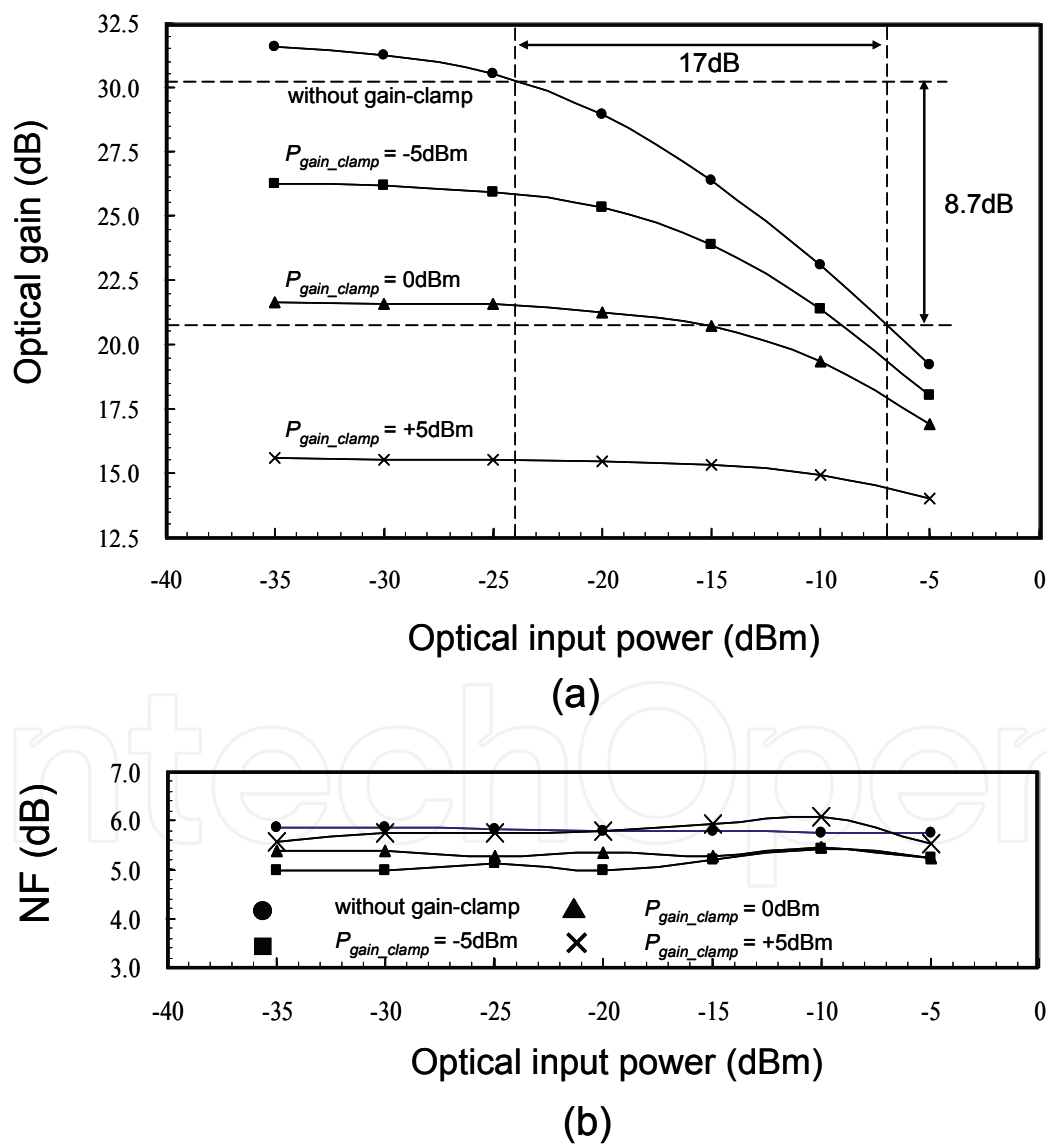


Fig. 9. (a) Optical gain (b) Noise figure as a function of optical input power; the parameter is the power of the gain-clamp light.

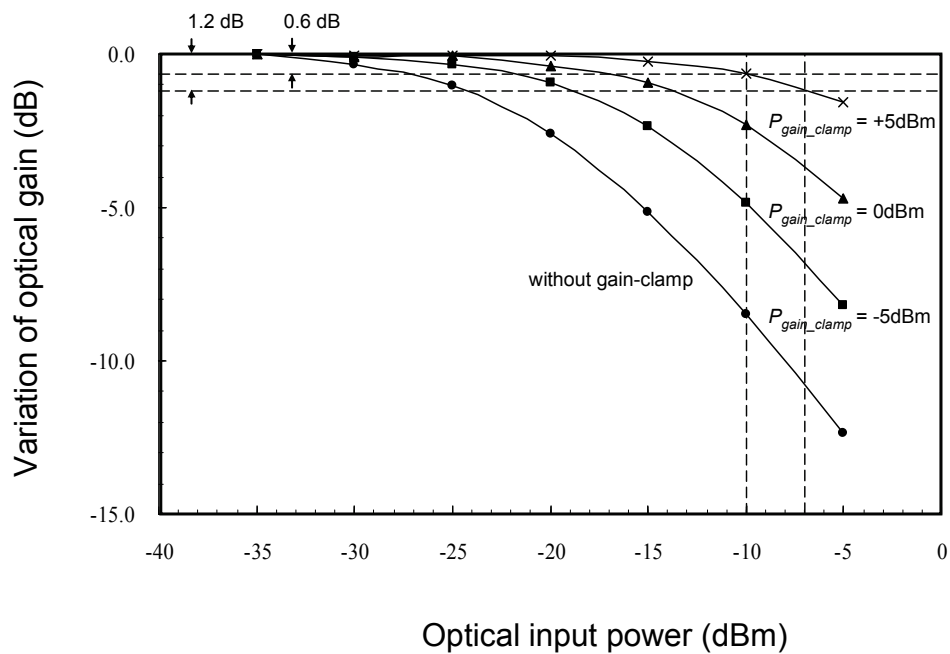


Fig. 10. Variation of optical gain as a function of optical input power; the parameter is the power of the gain-clamp light.

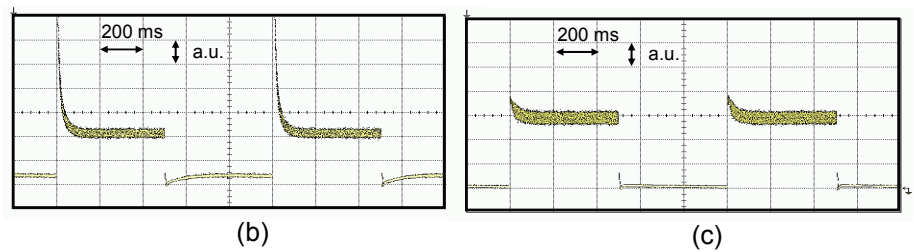
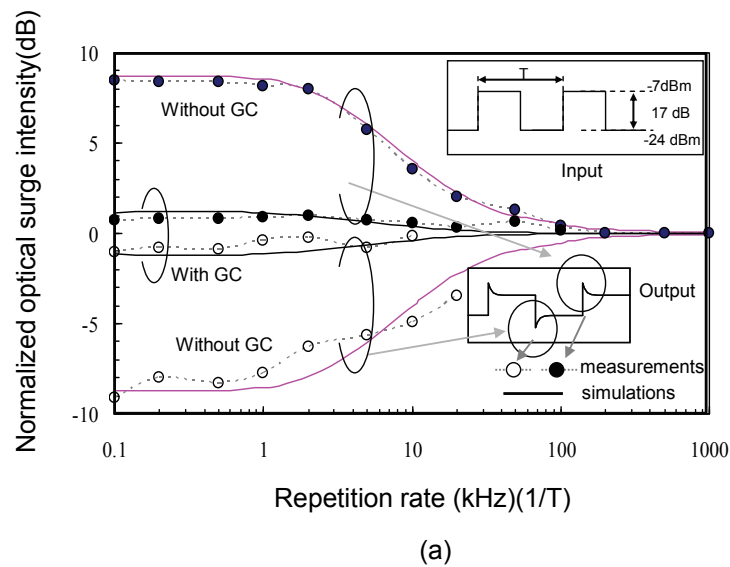


Fig. 11. (a) Numerical and measured results of normalized optical surge intensity as a function of burst repetition frequency. Examples of optical signal traces at repetition rate of 1 kHz (b) without GC and (c) with GC.

are often used to realize low noise figure operation and to control the output power, respectively. In this case, we fix both pump powers and use the gain-clamping system for gain control. Backward gain-clamping is chosen because it simplifies the separation of the gain-clamp light from the optical signals.

Figure 9 (a)-(b) show the optical gain and the noise figure (NF) as a function of optical input power; the parameter is the power of the gain-clamp light. Figure 10 shows the variation of optical gain as a function of optical input power; the parameter is the power of the gain-clamp light. Although gain-clamping causes gain suppression as shown in Fig. 9, we find that gain-clamping drastically improves PDFA linearity as shown in Fig. 10. In particular, a 1.2 dB gain variation and 14.4 dB gain are achieved when the gain-clamp power is 5 dBm and the input power range is below -7 dBm. Moreover, we can improve the gain variation and the gain to 0.6 dB and 15 dB, respectively, at input powers below -10 dBm.

Figures 11 (a)-(c) show the numerical and measured results of normalized optical surge intensity as a function of burst repetition frequency and typical optical signal traces at the repetition rate of 1 kHz with/without GC. Although residual optical surges are observed because of 1-dB gain compression power of -7 dBm, gain-clamping does improve the gain dynamic properties and can suppress optical surges as shown in Figs. 11 (a)-(c). Note that gain-clamping does not work well if the input power to the gain-clamped PDFA exceeds -7 dBm. For example, the splitting number must be above 4 when the ONU-PDFA distance is 7 km.

5. 10 Gbit/s burst-signal amplification using gain-clamped optical amplifier

5.1 Experimental setup of 10 Gbit/s burst-signal amplification

In this section, I focus on gain-clamp based burst-mode optical amplifiers (burst-AMP's) for 10 Gbit/s PON application to realize both long-reach and higher-speed PON systems. I then introduce the demonstration of 10 Gbit/s optical burst signal amplification to confirm their feasibility. Figure 12 shows the experimental setup for 10 Gbit/s optical burst-signal amplification; it consists of the burst-AMP under test, a burst-mode optical receiver (burst-Rx), a burst-mode optical transmitter 1 (burst-Tx1), and a burst-mode optical transmitter 2 (burst-Tx2). As the burst-AMP, we used our 0.98 μm pumped gain-clamped praseodymium-doped fiber amplifier (GC-PDFA) (K-I. Suzuki, et. al., 2007). This burst-AMP offers 17 dB gain and good gain linearity (the 1dB-gain compression power is -10 dBm). After the 3 nm optical band-pass filter (OBPF), optical gain is reduced to 16.2 dB by the 0.8 dB excess loss of the OBPF.

We used high-power with distributed feedback laser diodes (DFB-LD's) as burst-Tx's; they were directly modulated by 10.3125 Gbit/s signals with the pseudo random bit sequence (PRBS) 2^7-1 and $2^{23}-1$, to generate burst signal sequences. The transmission timing of each burst-Tx was controlled by the enable signals from the timing pulse generator that was synchronized to the pulse pattern generator and the bit-error rate tester. The 99.3 ns guard time was used to separate burst signal sequences and the 74.5 ns preamble (continuous "101010" signal) was used to set the threshold level of received electrical signals. Basically, the measured burst signal sequence was modulated with PRBS $2^{23}-1$ and the other burst signal sequence was modulated with PRBS 2^7-1 to distinguish them at the bit-error rate tester. So when we measured each burst signal sequence from the burst-Tx's, we replaced the PRBS patterns as required. The central wavelength, the averaged output power, and the extinction ratio of the burst Tx1 were 1303.0 nm, 5.6 dBm, and 9.6 dB, respectively. Those of the burst Tx2 were 1301.5 nm, 5.5 dBm, and 9.7 dB, respectively. Burst signal sequences

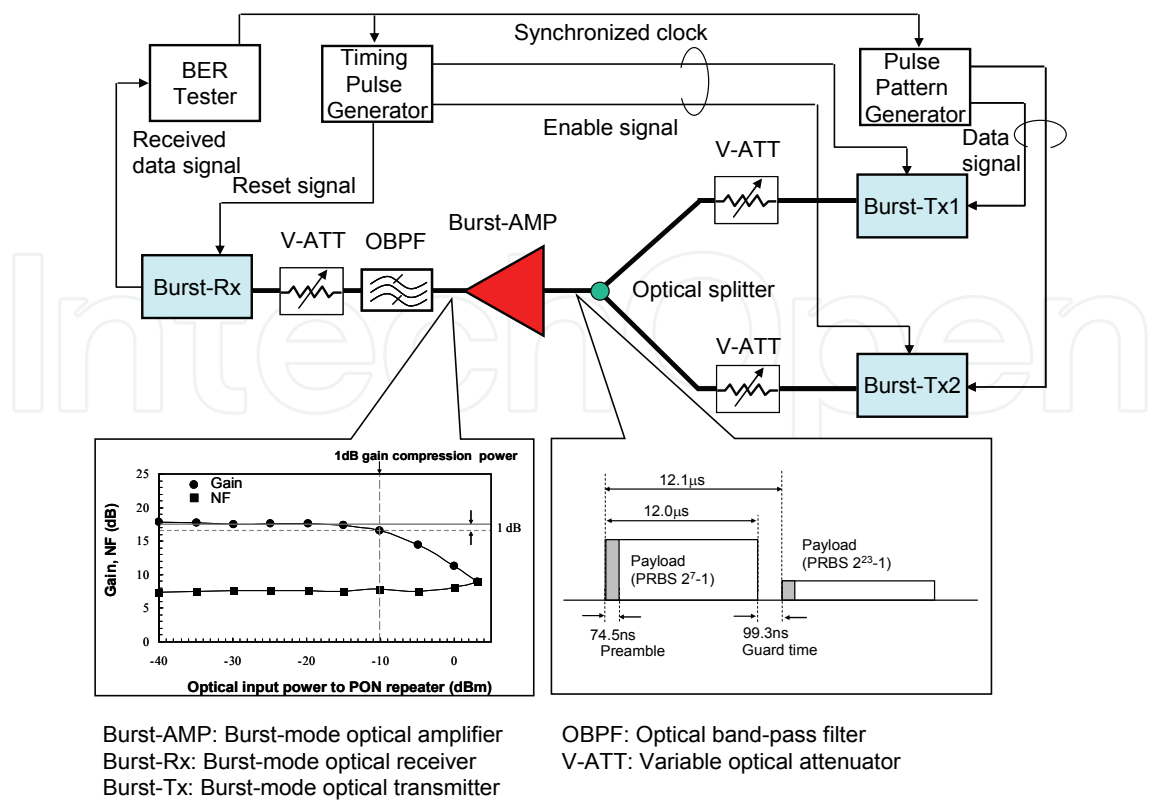


Fig. 12. Experimental setup for 10 Gbit/s burst signal amplification

with different intensities are generated by the variable attenuators (V-ATT) at the output of each burst-Tx. We set the link loss between the burst-AMP and burst-Tx1 and the burst Tx2 to 25.6 dB and 15.5 dB, so optical powers input to the burst-AMP were fixed at -20 dBm and -10 dBm, respectively. We varied the optical powers input to the burst-Rx to measure the allowable loss budget for 10 Gbit/s amplified PON systems. The burst-Rx consisted of a burst-mode limiting amplifier (burst-LIM) and a burst-mode trans-impedance amplifier (burst-TIA) (S. Nishihara, et. al., 2007) followed by an avalanche photodiode APD (T. Nakanishi, et. al., 2007). Its sensitivity (BER=10⁻¹²) and overload were estimated to be -22.2 dBm and -7.0 dBm, respectively, at the multiplication factor, M, of around 5.

5.2 Experimental results of 10 Gbit/s burst-signal amplification

Figure 13 shows the bit error rate (BER) as a function of averaged receive power to the burst-Rx. After the burst-AMP, we observed the power penalties, with and without the OBPF, of 1.2 dB and 2.2 dB, respectively, at BER=10⁻¹². On the other hand, at BER=10⁻⁴, the power penalties are reduced to within 1.0 dB. By the way, as IEEE P802.3av requires a 29 dB loss budget considering the use of forward error correction (FEC), we should also consider the FEC effect. Assuming the use of the FEC based on RS(255,239), which can improve the BER from 10⁻⁴ to 10⁻¹², we expect that FEC can improve the receiver sensitivity to -28.0 dBm Note that IEEE 802.3av adopted the RS(255, 223) based FEC, which can improve the BER from 10⁻³ to 10⁻¹², after this experiment..

Figures 14 (a) and (b) show the signal traces for the burst-AMP output and the burst-TIA output. As optical inputs to the burst-AMP were -20 dBm and -10 dBm, we obtained the optical output of -3.8 dBm and +5.2 dBm. After optical burst signal amplification, we did not observe any significant waveform degradation such as optical surges, see Fig.6-3 (a). On the

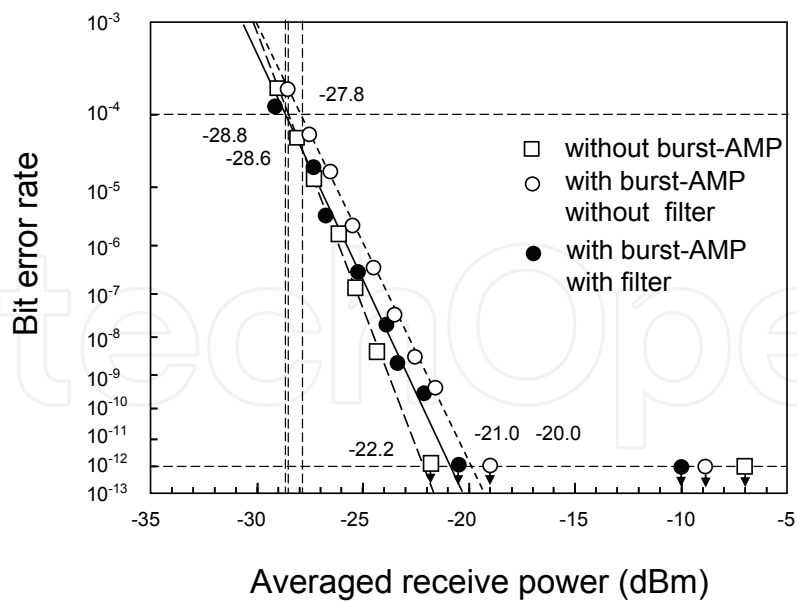


Fig. 13. BER as a function of averaged receive power to burst-Rx

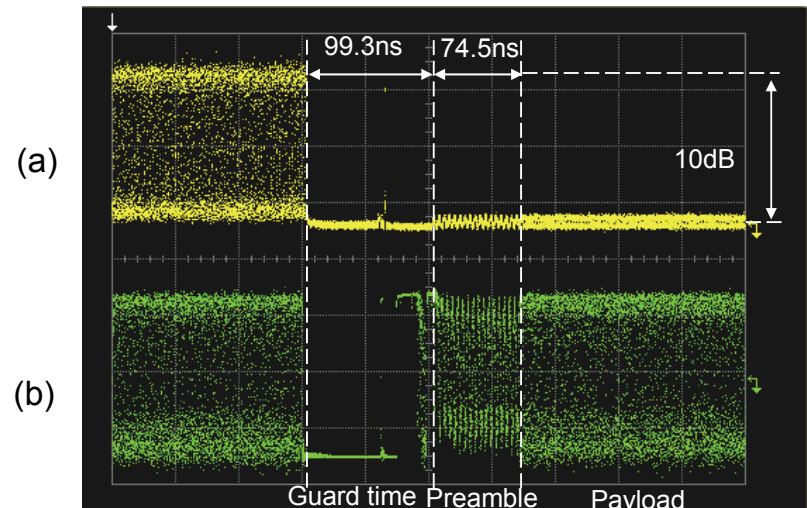


Fig. 14. Signal traces for (a) burst-AMP output and (b) burst-TIA output

other hand, received electrical signals were successfully regenerated within burst overhead time shown in Fig.14 (b).

Figure 15 shows the BER as a function of total loss. Not using the burst-AMP yields the estimated loss budget of 27.8 dB, which corresponds to 34.1 dB if FEC is used. On the other hand, when we use the burst-AMP, loss budget is improved to 42.6 dB, which corresponds to 50.4 dB when FEC is applied. Moreover, when we use the bust-AMP followed by the 3 nm OBPF, the loss budget is improved to 42.8 dB, which corresponds to 50.4 dB after FEC decoding. No significant difference is observed between cases of optical amplifier with/without the 3 nm OBPF, because the OBPF improves the receiver sensitivity but reduces the optical gain.

Therefore, we successfully achieved 15.0-dB improvement in the loss budget and a loss budget of 42.8 dB by using the burst-AMP. The use of FEC is expected to yield improvement values of 16.3 dB and 50.4 dB, respectively.

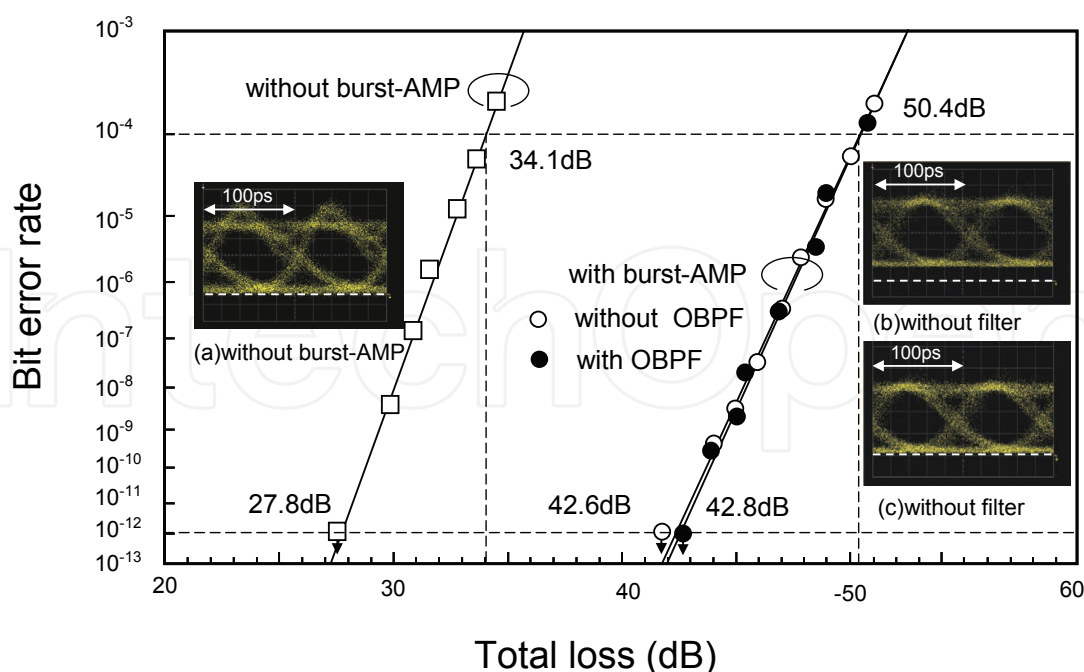


Fig. 15. Bit error rate as a function of total loss. Insets are eye patterns for optical signals (a) with burst AMP, (b) with burst-AMP without OBPF, and (c) with burst-AMP and OBPF

6. 10 Gbit/s burst-signal amplification using automatic level controlled burst-mode optical fiber amplifier

6.1 Automatic level controlled burst-mode optical fiber amplifier

To offer PON-based optical access services more effectively, we have investigated optically-amplified PON systems based on a couple of linear-gain control techniques, gain-clamping (GC) (K-I. Suzuki, et. al., 2007) and fast automatic gain controlling (fast AGC) for optical amplifiers (Y. Fukada, et. al., 2008, H. Nagaeda, et. al., 2008). In Section 5, we have introduced 10 Gbit/s optical burst signal amplification based on GC optical fiber amplifiers (OFA's) and confirmed their bit-rate independency. By the way, fast AGC techniques allow the linear gain region of OFA's to be expanded without gain suppression, GC techniques, on the other hand, are usually accompanied by considerable gain suppression. Accordingly, we expect AGC techniques will realize both higher linear gain and wider linear gain region (wider dynamic range). However, wide linear gain regions require that the burst-mode optical receivers (burst-Rx's) have wide dynamic range in order to take advantage of the fast AGC techniques.

In this section, I explain the optical automatic level control (ALC) techniques applied to fast AGC-OFA's to ease the requirements of the receiver's dynamic range. I then introduce the demonstration of 10 Gbit/s burst-RX based on the optical ALC techniques to confirm their feasibility.

Figure 16 shows the configuration of an ALC burst-mode OFA (burst-OFA); it consists of an AGC praseodymium-doped fiber amplifier (PDFA) block and an ALC circuit block. The AGC-PDFA employs a feed-forward (FF) controlled pump-LD for quick gain adjustment of the PDFA and offers constant gain of around 20 dB with optical input powers from -30 dBm to -10 dBm or above. The FF-controlled pump-LD quickly adjusts pump power according to the monitored signal power. The ALC circuit employs a FF-controlled variable optical

attenuator (VOA) for quick adjustment of output optical level and the suppression of waveform distortion caused by the gain dynamics of the AGC-PDF. Using these techniques, the ALC burst-OFA realizes quick ALC response, of the order of sub-micro-seconds, and offers the constant output optical level of around -17 dBm with optical input powers from -30 dBm to -10 dBm or above.

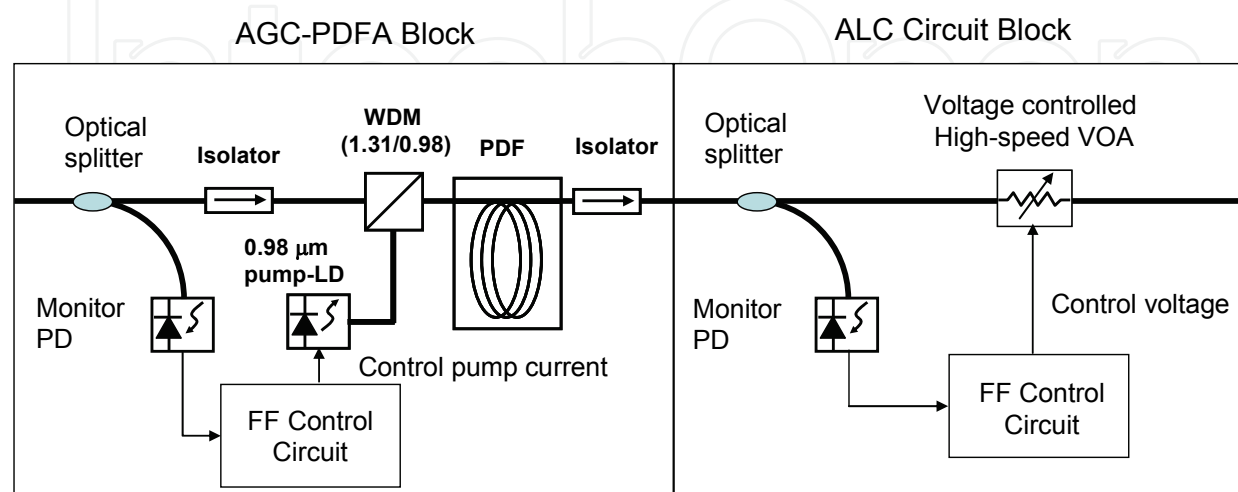


Fig. 16. Configuration of automatic level controlled burst-mode optical fiber amplifier

6.2 Experimental setup for bit-error rate measurement of 10 Gbit/s optically level controlled burst-signals

Figure 17 shows the experimental setup used to measure the bit-error rate (BER) of 10 Gbit/s optically level controlled burst-signals; the setup consists of a burst-Rx, a burst-mode optical transmitter 1 (burst-Tx1), and a burst-mode optical transmitter 2 (burst-Tx2). The burst-RX consists of the ALC-burst-OFA under test, a DC-coupled APD trans-impedance amplifier (APD-TIA), and a continuous-mode limiter amplifier (continuous LIM). We use a 3 nm band-pass filter (OBPF) for elimination of ASE noise from the ALC-burst-OFA. This reduces the optical output power of the ALC-burst-OFA to -18 dBm given the 1.0 dB excess loss of the OBPF.

We used DFB-LD's with quick response burst-mode LD drivers (H. Nakamura, et. al., 2008) as burst-TX's; they were directly modulated by 10.3125 Gbit/s signals with PRBS 27-1, to generate burst signal sequences. The transmission timing of each burst-Tx was controlled by the enable signals from the timing pulse generator that was synchronized to the pulse pattern generator and the BER tester. The 198.5 ns guard time was used to separate burst signal sequences and a part of the 496.4 ns preamble (continuous "101010" signal) was used to set the optical output level of the ALC-burst-OFA (Normally, it is used to set the threshold level of the burst-mode LIM). The central wavelength, the averaged output power, and the extinction ratio of the burst Tx1 were 1307.5 nm, 3.6 dBm, and 6.1 dB, respectively. Those of the burst Tx2 were 1306.9 nm, 4.2 dBm, and 6.2 dB, respectively. Burst signal sequences with different intensities were generated by the VOA's at the output of each burst-Tx. We varied the optical powers input to the burst-Rx and measured the BER to confirm the allowable dynamic range of our proposed ALC-burst-OFA.

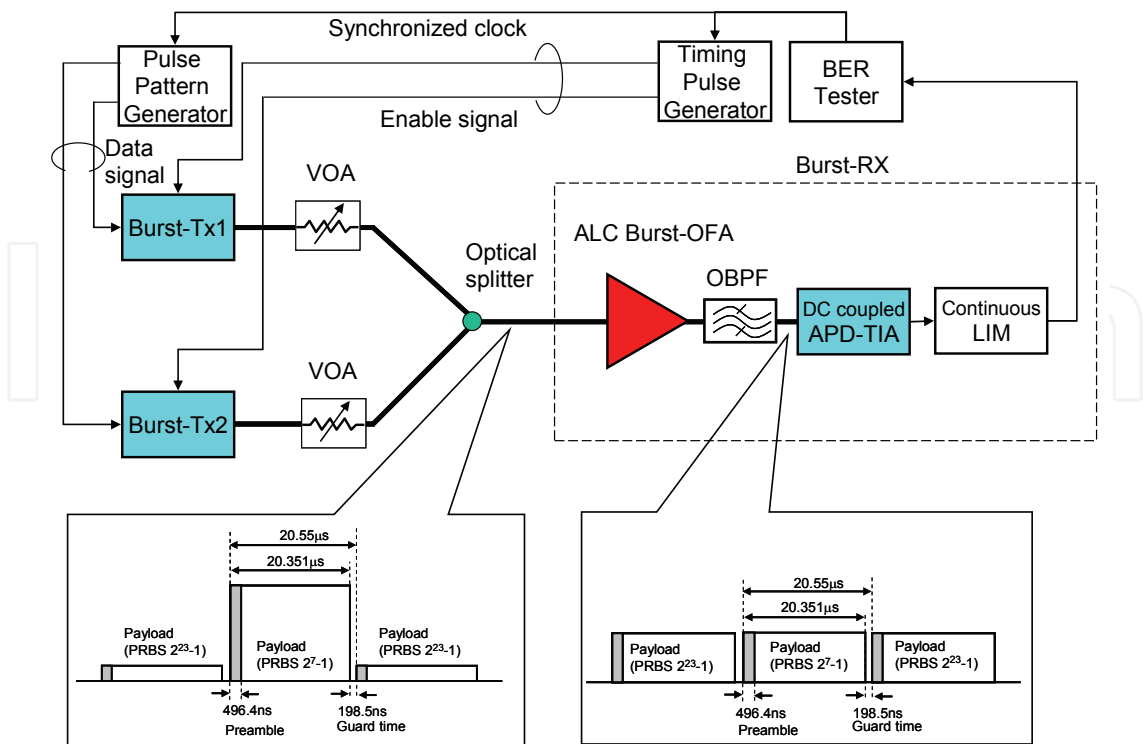


Fig. 17. Experimental setup for BER measurement of 10 Gbit/s burst signal

6.3 Experimental results of 10 Gbit/s burst-signal amplification

Figure 18 shows the signal traces for the ALC-burst-OFA inputs and outputs. We set the input power difference between burst-Tx's to 10.1 dB (Input powers from burst-Tx's were -20.3 dBm and -10.2 dBm), 19.7 dB (-29.9 dBm and -10.2 dBm), and 23.8 dB (-5.1 dBm and -28.9 dBm). As shown in Fig.18, the ALC-burst-OFA successfully achieved constant output level operation within the burst-overhead time; a small level difference was observed in Fig. 18(f).

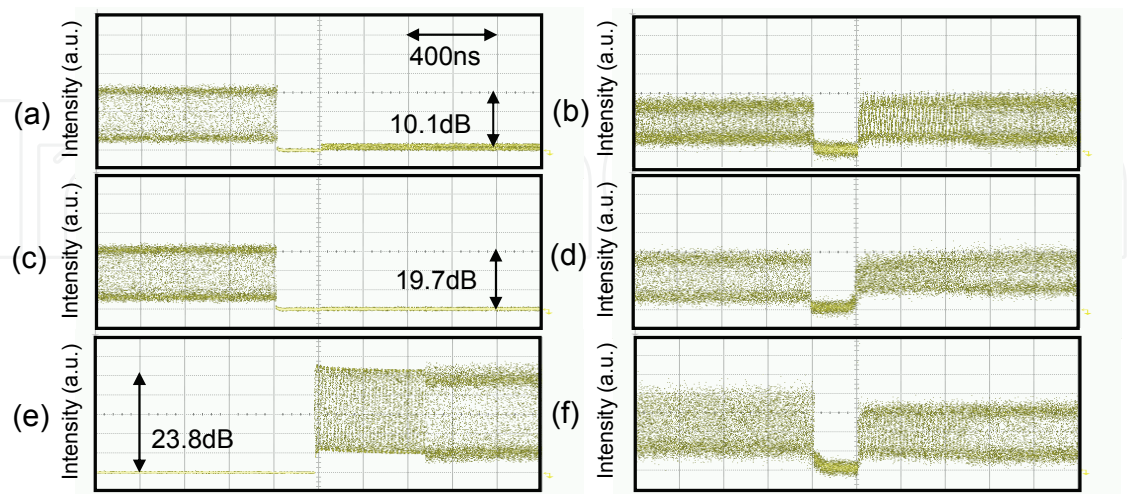


Fig. 18. Signal traces for ALC-burst-OFA inputs and outputs. (a)Input and (b) output signal traces at -20.3 dBm from burst-Tx1 and -10.2dBm from burst-Tx2. (c) Input and (d) output signal traces at -29.9 dBm and -10.2dBm. (e) Input and (f) output signal traces at -5.1 dBm and -28.9dBm.

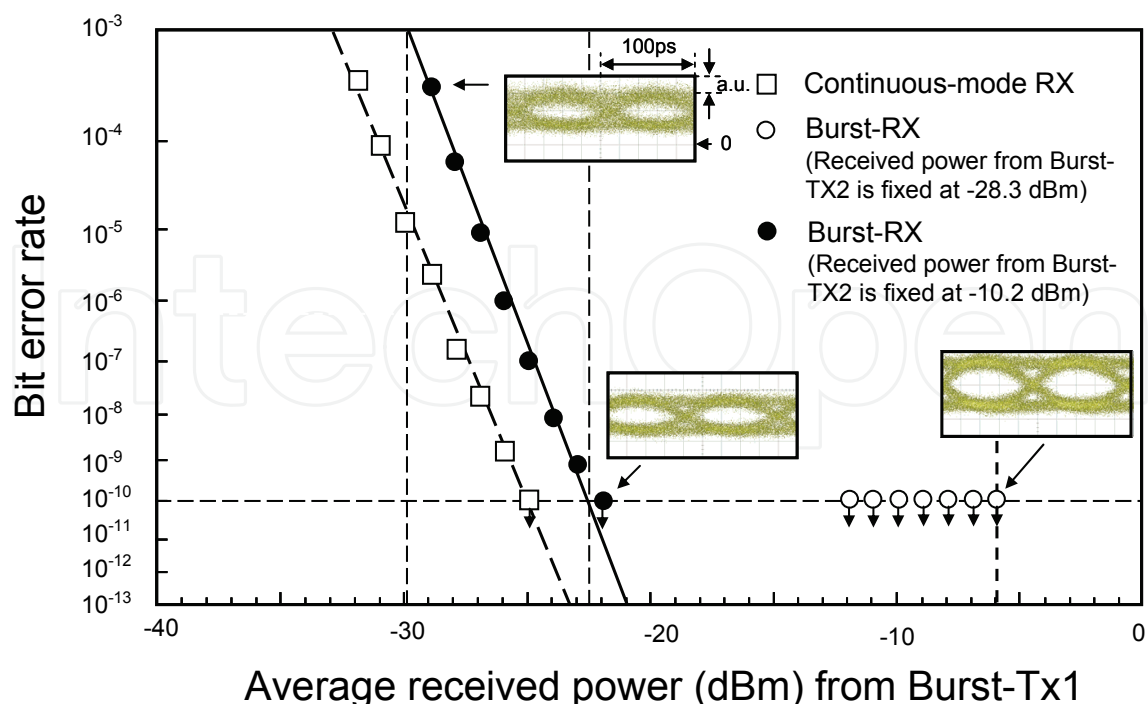


Fig. 19. Bit error rate as a function of averaged received power from Burst-TX1. Insets are eye patterns for optical signals.

Figure 19 shows the BER as a function of averaged received power to the burst-Rx at fixed received power from the burst-Tx2 (-28.3 dBm and -10.2 dBm). We also show the BER curve of the continuous-mode Rx for comparison; it consisted of a burst-mode (DC-coupled) APD-TIA and a continuous-mode LIM followed by continuous-mode PDFA. The receiver sensitivity was -22.5 dBm at $\text{BER}=10^{-10}$; the power penalty relative to the continuous-mode device was 2.6 dB. However, our ALC-burst-OFA successfully achieved a dynamic range of over 16.6 dB at $\text{BER}=10^{-10}$, thus confirming its feasibility in easing the receiver dynamic range requirement. By the way, as IEEE 802.3av requires a 29 dB loss budget considering the use of forward error correction (FEC), we should also consider the FEC effect. Assuming the use of FEC based on RS(255,223), which can improve the BER from 10^{-3} to 10^{-12} , we expect that FEC will improve the receiver sensitivity and the dynamic range to -29.7 dBm and 23.8 dB, respectively.

7. Conclusion

I introduced burst-mode optical amplifiers for PON systems based on a couple of linear-gain control techniques, gain-clamping (GC), fast automatic gain controlling (fast AGC), and fast automatic level controlling (fast ALC) for optical amplifiers. I also investigated the gain dynamics of a gain-clamped PDFA for achieving burst mode amplification and confirmed the ability of gain-clamping to suppress optical surges. I also investigated the validity of a gain-clamped PDFA for burst mode amplification by estimating the transmission distance and the allowable splitting number of Long-reach PON systems.

Moreover, I also introduced the demonstration of 10 Gbit/s optical burst signal amplification based on GC based optical fiber amplifiers (OFA's) and optical automatic level control (ALC) techniques applied to fast to ease the requirements of the receiver's dynamic

range to confirm their feasibility. Using GC based OFA's, we successfully achieved a 15.0 dB improvement in the loss budget, which stands at over 42.8 dB loss budget, by using the burst-mode optical amplifier based on gain-clamping. Moreover, the application of FEC can improve those results to 16.3 dB and 50.4 dB, respectively. No significant difference was observed between the cases of the GC based OFA with/without the optical band-pass filter. These results confirm the validity of the GC based OFA for 10 Gbit/s PON systems.

Using ALC based OFA's, we successfully received burst signals with 198.5 ns guard time and 496.4 ns preamble, and achieved a dynamic range of over 16.6 dB and receiver sensitivity of -22.5 dBm at BER=10⁻¹⁰ by combining our ALC based OFA, a DC-coupled APD trans-impedance amplifier, and a continuous-mode limiter amplifier; the results confirm the feasibility of our ALC based OFA in 10 Gbit/s PON systems.

8. References

- H. Shinohara, "FTTH experiences in Japan", JON 6, pp. 616-623 (2007).
- K-I. Suzuki, T. Furukawa, K. Saito, and H. Ueda, "Role and development of B-PON regenerator", OHAN2002 paper 4.4, pp.115-121(2002) or "B-PON repeater for enlarging transmission distance between OLT and ONT", IEICE Transaction of Information and Communication Engineers B, vol.J86-B no.10, pp.2053-2064 (2003).
- ITU-T Recommendation G.983, G.984, and G.987 series
- IEEE Standard 802.3ah, 802.3av, IEEE P1904.1
- K-I. Suzuki, Y. Fukada, D. Nasset, and R. Davey, "Amplified gigabit PON systems", JON 6, 422-433 (2007).
- R. Davey, D. Grossman, M. Rasztovits-Wiech, D. Payne, D. Nasset, A. Kelly, A. Rafel, S. Appathurai, and S. Yang, "Long-reach passive optical networks", J. Lightwave Technol. Vol.27, No.3, pp.273-291(2009).
- Z. Belfqih, P. Chanclou, F. Saliou, N. Genay and B. Landousies, "Enhanced Optical Budget System Performance of an Burst Extended PON at 10.7 Gbit/s over 60 km of Fiber". ECOC'2008, paper Th.2.F.4, Brussel, Belgium, September, 2008.
- F. Saliou, P. Chanclou, F. Laurent, N. Genay, J. Lazaro, F. Bonada, and J. Prat, "Reach Extension Strategies for Passive Optical Networks", J. Opt. Commun. Netw., Vol. 1, No. 4, C51-C-60(2009).
- ITU-T Recommendation G.984.6, "Gigabit-capable passive optical networks (GPON): Reach extension", (2008).
- H. Ueda and E. Maekawa, "Development of an ATM subscriber system (Model C)", NTT Review 11, 6, pp.27-32 (1999).
- Gerlas van den Hoven, "Linear optical amplifier", LEOS2002 paper ThCC2.
- K-I. Suzuki, Y. Fukada, D. Nasset, and R. Davey, "Amplified gigabit PON systems", J. Optical Networking, Vol. 6, no. 5, 422-433 (2007).
- Y. Fukada, K-I. Suzuki, H. Nakamura, N. Yoshimoto, and M. Tsubokawa, "First demonstration of fast automatic-gain-control (AGC) PDFA for amplifying burst-mode PON upstream signal", ECOC 2008, papwer We.2.F.4.
- H. Nagaeda, Y. Horiuchi, Y. Tanaka, N. Shiga, Y. Fukada, K-I. Suzuki, N. Yoshimoto, and M. Tsubokawa, "Burst-mode optical amplifier for signals with various burst length from 500 ns to 50 ms", ECOC 2008, paper P.1.13.
- K-I. Suzuki, Y. Fukada, K. Saito, and Y. Maeda, "Long-reach PON System using Gain-clamped Optical Amplifier", WTC2006, paper NT3 #2.

- K-I. Suzuki, Y. Fukada, T. Nakanishi, N. Yoshimoto, and M. Tsubokawa, "Burst-mode optical amplifier for long-reach 10 Gbit/s PON application", OFC2008, paper OthL3.
- K-I. Suzuki, Y. Fukada, N. Yoshimoto, K. Kumozaki, M. Tsubokawa, "Automatic Level Controlled Burst-Mode Optical Fiber Amplifier for 10 Gbit/s PON Application", OFC 2009, paper OTuH1.
- N. A. Olsson, "Lightwave systems with optical amplifier", IEEE Journal of Lightwave Technol., vol. 7, no. 7, pp.1071-1082, July 1989.
- N. S. Bergano, F. W. Kerfoot, and C. R. Davidson, "Margin measurement in optical amplifier system", IEEE Photon. Technol. Lett., vol. 5, no. 3, pp. 304-306, March 1993.
- T. Takahashi, M. Aoyama, M. Murakami, and M. Amemiya, "Modeling of intersymbol interference effect on signal to noise ratio measurement in long haul optical amplifier systems", Electron. Lett., vol.31, pp. 2195-2197, 1995.
- H. Masuda, K.-I. Suzuki, S. Kawai, and K. Aida, "Ultra-wideband optical amplification with 3dB bandwidth of 65 nm using a gain equalized two-stage erbium-doped fiber amplifier and Raman amplification", Electron. Lett., vol.33, no.9 pp.753-754, April 1997.
- L. L. Yi, L. Zhan, Q. H. Ye, X. Hu, and Y. X. Xia, "Gain-clamped erbium-doped fiber-ring lasing amplifier with low noise figure by using an interleaver", IEEE Photon. Technol. Lett., vol.15, no.12, pp.1695-1697, December 2003.
- Yung-Hsin Lu and Sien Chi, "Two-stage L-band EDFA applying C/L-band wavelength-division multiplexer with the counterpropagating partial gain-clamping", IEEE Photon. Technol. Lett., vol.15, no.12, pp.1710-1712, December 2003.
- D. A. Francis, S. P. DiJaili, and J.D. Wallker, "A single-chip linear optical amplifier", OFC2001 PDP13-1.
- S. Nishihara, S. Kimura, T. Yoshida, M. Nakamura, J. Terada, K. Nishimura, K. Kishine, K. Kato, Y. Ohtomo, and T. Imai, "A 10.3125-Gbit/s SiGe BiCMOS Burst-Mode 3R Receiver for 10G-EPON Systems," OFC2007 PDP8.
- S. Nishihara, M. Nakamura, K. Nishimura, K. Kishine, S. Kimura, and K. Kato, "A fast-response and high-sensitivity PIN-TIA module with wide dynamic range for 10G burst-mode transmissions", ECOC2007 paper 4.4.1.
- T. Nakanishi, K-I. Suzuki, Y. Fukada, N. Yoshimoto, M. Nakamura, K. Kato, K. Nishimura, Y. Ohtomo, and M. Tsubokawa, "High sensitivity APD burst-mode receiver for 10Gbit/s TDM PON system", IEICE Electronics Express 4, 588-592 (2007).
- H. Nakamura, S. Kimura, K. Hara, N. Yoshimoto, M. Tsubokawa, M. Nakamura, K. Nishimura, A. Okada, and Y. Ohtomo, "500-ps response AC-coupled burst-mode Transmitter using baseline-wander common-mode rejection technique for 10-Gbit/s-class PON system", OFC2008, paper PDP26.



Advances in Optical Amplifiers

Edited by Prof. Paul Urquhart

ISBN 978-953-307-186-2

Hard cover, 436 pages

Publisher InTech

Published online 14, February, 2011

Published in print edition February, 2011

Optical amplifiers play a central role in all categories of fibre communications systems and networks. By compensating for the losses exerted by the transmission medium and the components through which the signals pass, they reduce the need for expensive and slow optical-electrical-optical conversion. The photonic gain media, which are normally based on glass- or semiconductor-based waveguides, can amplify many high speed wavelength division multiplexed channels simultaneously. Recent research has also concentrated on wavelength conversion, switching, demultiplexing in the time domain and other enhanced functions. *Advances in Optical Amplifiers* presents up to date results on amplifier performance, along with explanations of their relevance, from leading researchers in the field. Its chapters cover amplifiers based on rare earth doped fibres and waveguides, stimulated Raman scattering, nonlinear parametric processes and semiconductor media. Wavelength conversion and other enhanced signal processing functions are also considered in depth. This book is targeted at research, development and design engineers from teams in manufacturing industry, academia and telecommunications service operators.

How to reference

In order to correctly reference this scholarly work, feel free to copy and paste the following:

Ken-Ichi Suzuki (2011). Burst-Mode Optical Amplifiers for Passive Optical Networks, *Advances in Optical Amplifiers*, Prof. Paul Urquhart (Ed.), ISBN: 978-953-307-186-2, InTech, Available from:
<http://www.intechopen.com/books/advances-in-optical-amplifiers/burst-mode-optical-amplifiers-for-passive-optical-networks>

INTECH
open science | open minds

InTech Europe

University Campus STeP Ri
Slavka Krautzeka 83/A
51000 Rijeka, Croatia
Phone: +385 (51) 770 447
Fax: +385 (51) 686 166
www.intechopen.com

InTech China

Unit 405, Office Block, Hotel Equatorial Shanghai
No.65, Yan An Road (West), Shanghai, 200040, China
中国上海市延安西路65号上海国际贵都大饭店办公楼405单元
Phone: +86-21-62489820
Fax: +86-21-62489821

© 2011 The Author(s). Licensee IntechOpen. This chapter is distributed under the terms of the [Creative Commons Attribution-NonCommercial-ShareAlike-3.0 License](https://creativecommons.org/licenses/by-nc-sa/3.0/), which permits use, distribution and reproduction for non-commercial purposes, provided the original is properly cited and derivative works building on this content are distributed under the same license.

IntechOpen

IntechOpen